Supporting Information for

Superstructures with Diverse Morphologies and Highly Ordered Fullerene C_{60} Arrays from 1:1 and 2:1 Adamantane-C_{60} Hybrid Molecules

Shengju Zhou,[a,d] Lin Wang,[b] Mengjun Chen,[c] Baoyong Liu,[a,d] Xiaofeng Sun,[a,d] Meirong Cai,[a] Hongguang Li,[a]*

[a]*State Key Laboratory of Solid Lubrication & Laboratory of Clean Energy Chemistry and Materials, Lanzhou Institute of Chemical Physics, Chinese Academy of Sciences, Lanzhou, Gansu Province, 730000, China*

[b] *Analytical center of Qilu Normal University, Jinan, Shandong Province, 250200, China*

[c]*Key Laboratory of Colloid and Interface Chemistry & Key Laboratory of Special Aggregated Materials, Shandong University, Ministry of education, Jinan, Shandong Province, 250100, China*

[d] *University of Chinese Academy of Sciences, Beijing, 100049, China*

1. Syntheses

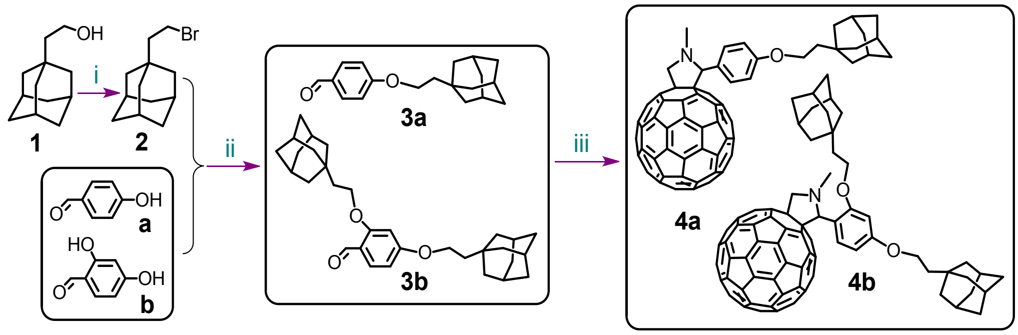

Scheme S1 Synthetic route for Ad-C_{60} hybrid molecules. i) CBr_4, PPh_3, THF, r.t., 0.5 h. ii) K_2CO_3, DMF, 120 °C, overnight. iii) C_{60}, sarcosine, chlorobenzene, 140 °C, overnight.

1.1. Synthesis of 1-bromo-2-adamantaneethane (2)

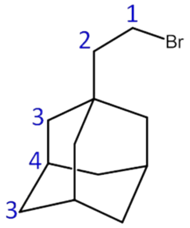

To a 50 mL two-neck round bottom flask, 1.5045 g (8.35 mmol) 1-adamantaneethanol, 4.9708 g (18.97 mmol) PPh_3, and 4.0337g CBr_4 (12.31 mmol) were added. After removing the air by repeated vacuum-argon cycles (×3), 25 mL anhydrous THF was injected and the mixture was stirred at room temperature for 30 min. Then the excess PPh_3 and CBr_4 were filtered off. The solvent was removed under reduced pressure and hexane was added. The mixture was filtered to remove the insoluble byproduct. The solvent was removed under reduced pressure and the resulting crude product was purified by silica gel column chromatography using hexane as an eluent. The final product was obtained as a white solid. (1.1083 g, yield: 54.83% based on the conversion of 1-adamantaneethanol). ^{1}H NMR (400 MHz, $CDCl_3$): δ 3.43-3.38 (t, 2H, *1*), 1.96 (s, 3H, *4*), 1.74-1.51 (m, 14H, *2 and 3*). MALDI-TOF-MS calculated: 242.07, Found: 242.35.

1.2. Synthesis of Ad-substituted benzaldehyde (3a and 3b)

*Synthesis of **3a**.*

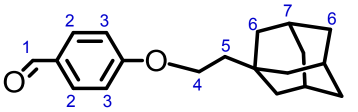

To a 50 mL two-neck flask, 0.1254 g (1.03 mmol) 4-hydroxybenzaldehyde and 0.1457 g (1.06 mmol) K_2CO_3 were added. After removing the air by repeated vacuum-argon cycles (×3), 10 mL anhydrous DMF was injected and the mixture was stirred at room temperature to make a homogeneous suspension. Then, 10 mL anhydrous DMF with pre-dissolved 0.2499 g (1.03 mmol) **2** was injected and the mixture was stirred at 70 °C for 17h. After cooled to room temperature, the mixture was concentrated under vacuum. The residue was dissolved in $CHCl_3$, washed successively with water (×3) and brine (×1) in a separatory funnel. The organic layer was combined, dried over anhydrous Na_2SO_4, and concentrated under reduced pressure. The crude product was subjected to silica gel column chromatography using hexane/$CHCl_3$ (40/60 v/v) mixture as the eluent. After that, some impurities still exist, the mixture was subjected to silica gel column chromatography again using hexane/$CHCl_3$ (30/70 v/v) mixture as the eluent. The final product was obtained as a white solid. (0.1843 g, yield: 63.0% based on the conversion of 4-hydroxybenzaldehyde). ^1H NMR (400 MHz, $CDCl_3$): δ 9.88 (s, 1H, *1*), 7.84-7.81 (d, 2H, *2*), 7.00-6.97 (d, 2H, *3*), 4.13-4.09 (t, 2H, *4*), 1.98 (s, 3H, *7*), 1.74-1.59 (m, 14H, *5 and 6*). ESI-MS Calculated: 284.18; Found $[M+H]^+$: 285.19.

Synthesis of ***3b***.

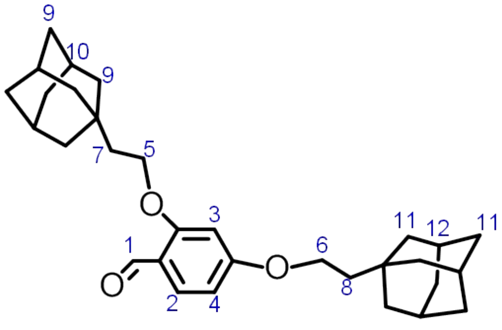

To a 50 mL two-neck flask, 0.0648 g (0.47 mmol) 2,4-dihydroxybenzaldehyde and 0.1620 g (1.17 mmol) K_2CO_3 were added. After removing the air by repeated vacuum-argon cycles (×3), 10 mL anhydrous DMF was injected and the mixture was stirred at room temperature to make a homogeneous suspension. Then, 10 mL anhydrous DMF with pre-dissolved 0.2522 g (1.04 mmol) **2** was injected and the mixture was stirred at 70 °C for 17 h. After cooled to room temperature, excess K_2CO_3 was removed by filtration and the mixture was concentrated under vacuum. The residue was dissolved in $CHCl_3$, washed successively with water (×3) and brine (×1). The organic layer was combined, dried over anhydrous Na_2SO_4, and concentrated under reduced pressure. The crude product was subjected to silica gel column chromatography using hexane/$CHCl_3$ (40/60 v/v) mixture as the eluent. After that, some impurities still exist, the mixture was subjected to silica gel column chromatography again using hexane/$CHCl_3$ (30/70 v/v) mixture as the eluent. The final product was obtained as a white solid. (0.1714 g, yield: 78.88% based on the conversion of 2,4-dihydroxybenzaldehyde). ^{1}H NMR (400 MHz, $CDCl_3$): δ 10.31 (s, 1H, *1*), 7.81-7.79 (d, 1H, *2*), 6.52-6.50 (m, 1H, *4*), 6.41-6.40 (d, 1H, *3*), 4.12-4.07 (m, 4H, *5 and 6*), 1.96-1.95 (d, 6H, *10 and 12*), 1.74-1.59 (m, 28H, *7, 8, 9 and 11*). ESI-MS Calculated: 462.31; Found $[M+H]^+$: 463.32.

1.3. Synthesis of N-Methylfulleropyrrolidines Bearing Adamantane Group (4a and 4b)

*Synthesis of **4a**.*

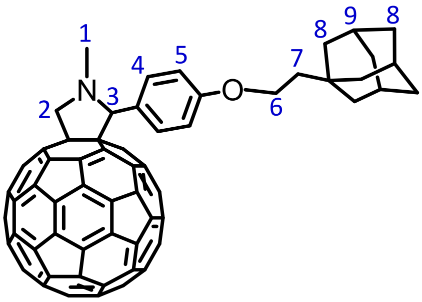

To a 500 mL two-neck round bottom flask, 0.7054 g C_{60} (0.98 mmol) and 0.2854 g sarcosine (3.20 mmol) were added. After removing the air by repeated vacuum-argon cycles (×3), 300 mL chlorobenzene was injected to make a homogeneous suspension. Then, 100 mL chlorobenzene containing 0.1843 g (0.65 mmol) **3a** was injected and the mixture was stirred at 140 °C overnight. After cooled to room temperature, excess sarcosine was removed by filtration and the organic solvent was removed under reduced pressure. The residue was dissolved in toluene and passed through a short silica gel column. The effluent was combined, concentrated under reduced pressure and redissolved in toluene. After further purification by gel permeation chromatography (GPC, Bio-Beads S-X1, 200-400 mesh) using toluene as an eluent, the final product was obtained as a brown solid (0.2633 g, yield: 33.49% based on the conversion of ***3a***, and 22.22% based on the conversion of C_{60}). ^{1}H NMR (400MHz, $CDCl_3$): δ 7.73 (s, 2H, *4*), 6.97-6.94 (d, 2H, *5*), 5.07-4.98 (d, 2H, *2*), 4.32-4.29 (d, 1H, *3*), 4.05-4.00 (t, 2H, *6*), 2.86 (s, 3H, *1*), 1.96 (s, 3H, *9*), 1.73-1.61 (m, 14H, *7 and 8*). ^{13}C NMR (400MHz, $CDCl_3$): δ 151.88, 147.37, 146.33, 146.25, 146.19, 146.17, 146.15, 145.97, 145.94, 145.81, 145.52, 145.40, 145.34, 145.30, 145.29, 145.21, 144.74, 144.64, 144.53, 144.51, 144.39, 144.38, 144.23, 144.06, 144.02, 143.16, 143.00, 142.62, 142.60, 142.59, 142.26, 142.22, 142.19, 142.09, 142.05, 141.99, 141.68, 140.19, 140.14, 139.93, 139.62, 135.74, 130.64, 117.78, 114.82, 99.98, 83.32, 77.19, 64.06, 43.05, 42.72, 37.07, 29.68, 28.66. MALDI-TOF-MS calculated: 1031.22, Found: 1031.46.

Synthesis of ***4b****.*

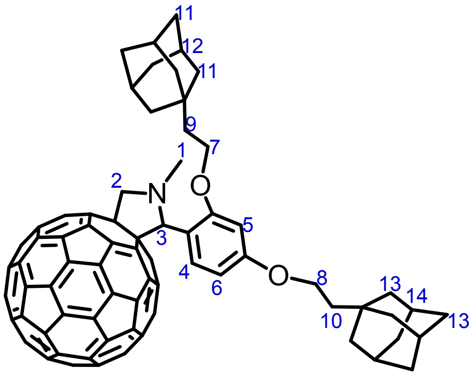

To a 500 mL two-neck round bottom flask, 0.4062g C_{60} (0.56 mmol) and 0.1704 g sarcosine (1.91 mmol) were added. After removing the air by repeated vacuum-argon cycles (×3), 300 mL chlorobenzene was injected to make a homogeneous suspension. Then, 100 mL chlorobenzene containing 0.1714 g (0.37 mmol) **3b** was injected and the mixture was stirred at 140 °C overnight. After cooled to room temperature, excess sarcosine was removed by filtration and the organic solvent was removed under reduced pressure. The residue was dissolved in toluene and passed through a short silica gel column. The effluent was combined, concentrated under reduced pressure and redissolved in toluene. Further purification by gel permeation chromatography (GPC, Bio-Beads S-X1, 200-400 mesh) using toluene as an eluent, the final products were obtained as brown solids (0.1902 g, yield: 42.51% based on the conversion of ***3b***, and 28.08% based on the conversion of C_{60}). ^{1}H NMR (400MHz, $CDCl_3$): δ 7.82-7.80 (d, 1H, *4*), 6.60-6.57 (m, 1H, *5*), 6.46-6.45 (d, 1H, *6*), 4.97-4.95 (d, 1H, J=8 Hz *2*), 4.28-4.26 (d, 1H, J=8 Hz *2*), 5.46 (s, 1H, *3*), 4.09-4.00 (m, 4H, *7 and 8*) 2.79 (s, 3H, *1*), 1.96-1.95 (d, 6H, *12 and 14*), 1.73-1.59 (m, 28H, *9, 10, 11 and 13*). ^{13}C NMR (400MHz, $CDCl_3$): δ 159.90, 158.75, 147.29, 146.89, 146.86, 146.60, 146.24, 146.17, 146.09, 146.06, 145.94, 145.78, 145.68, 145.55, 145.54, 145.29, 145.27, 145.23, 145.09, 145.08, 145.06, 144.61, 144.56, 144.53, 144.37, 143.05, 142.99, 142.63, 142.57, 142.54, 142.35, 142.23, 142.19, 142.12, 142.10, 141.99, 141.92, 141.72, 141.71, 141.58, 140.17, 140.10, 139.63, 139.48, 136.61, 136.18, 134.482, 117.62, 105.40, 99.74, 83.18, 75.61, 69.95, 69.21, 64.20, 64.03, 43.13, 42.78, 42.71, 41.04, 40.14, 37.06, 31.85, 31.62, 29.70, 28.65. MALDI-TOF-MS calculated: 1209.36, Found: 1210.30

2. Additional data

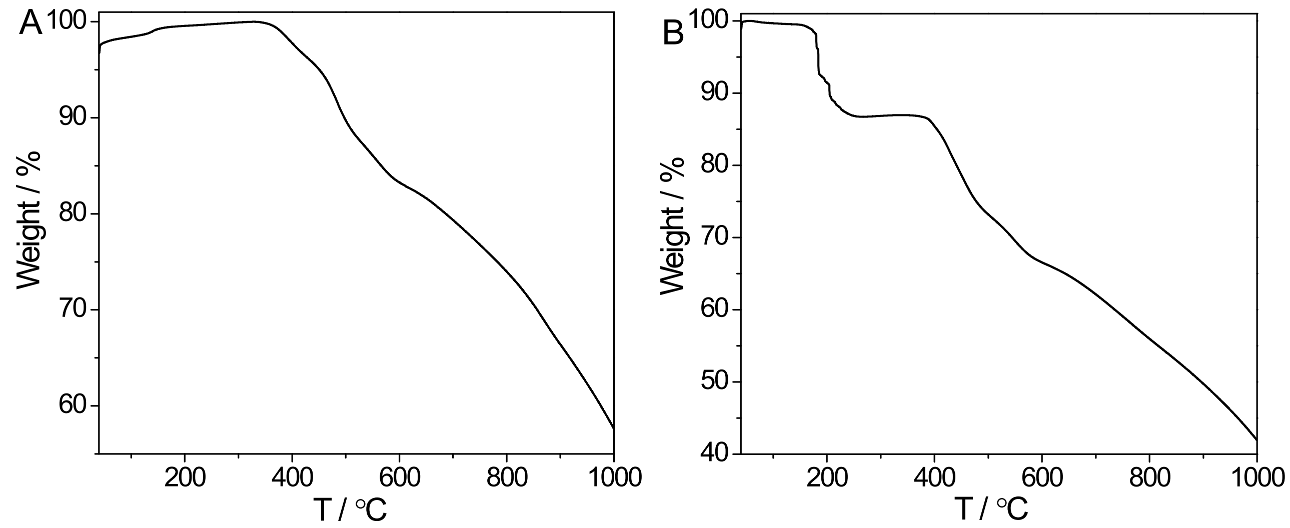

Fig. S1 TGA curves of **4a** (A) and **4b** (B).

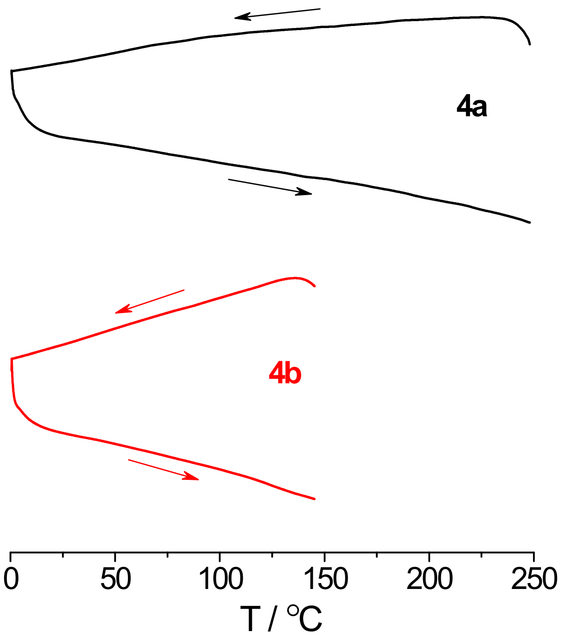

Fig. S2 DSC traces of **4a** and **4b** from the second heating-cooling circle. No melting point can be detected below their decomposition temperature.

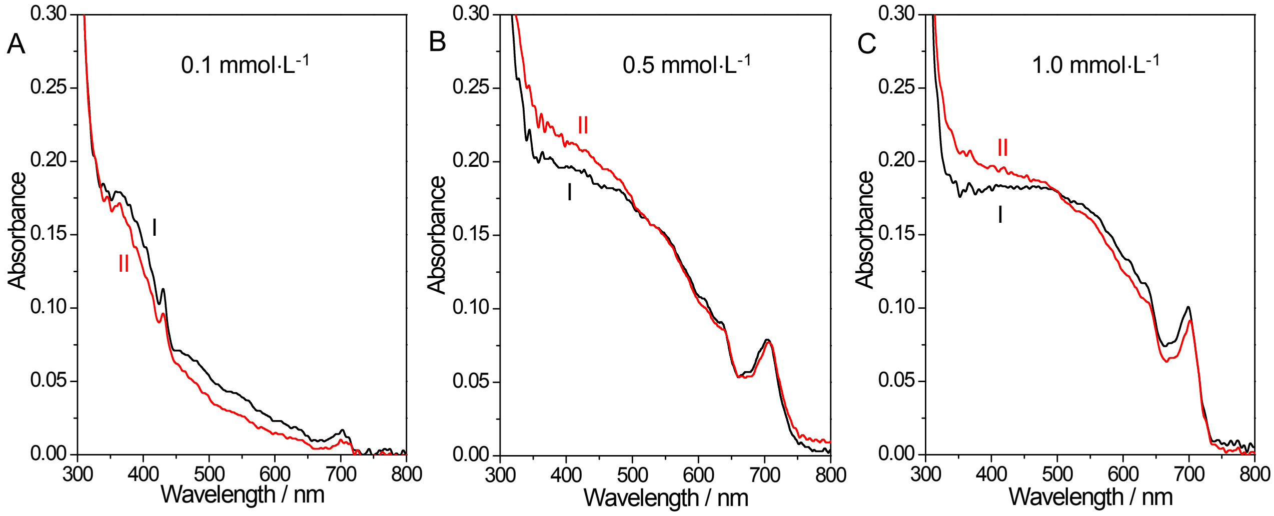

Fig. S3 UV-vis absorption of **4a** (I) and **4b** (II) in $CHCl_3$ at various concentrations as indicated.

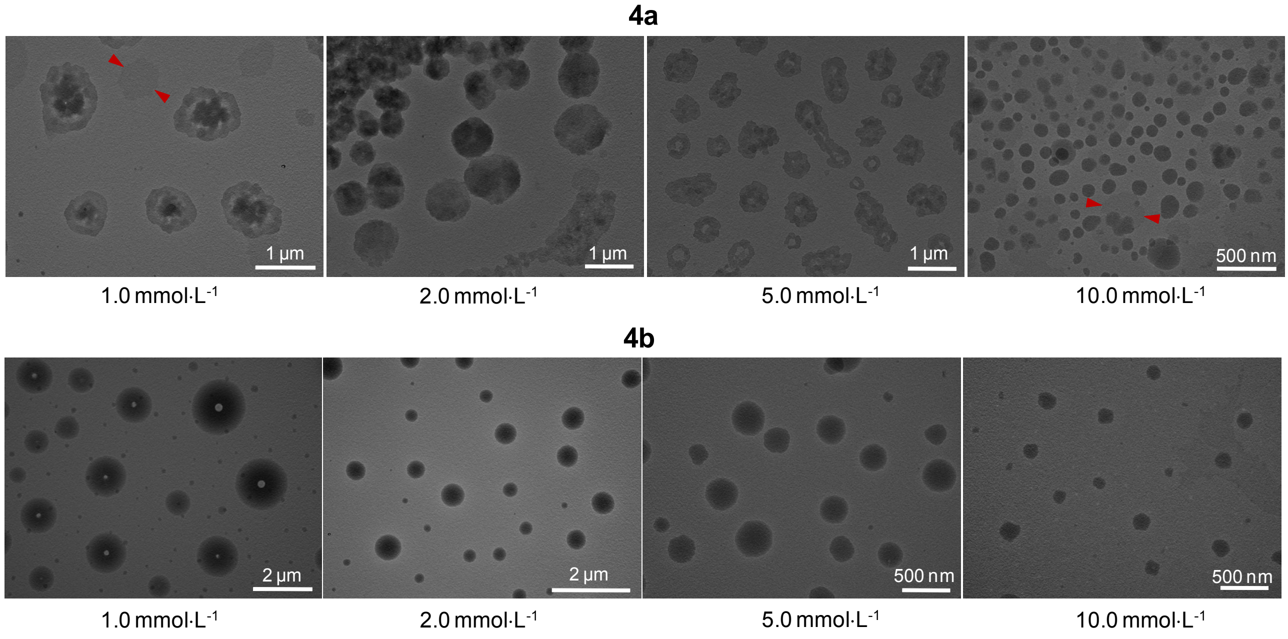

Fig. S4 Typical TEM images of **4a** and **4b** in $CHCl_3$ at selected concentrations. The presence of thin plates have been indicated between the arrow heads.

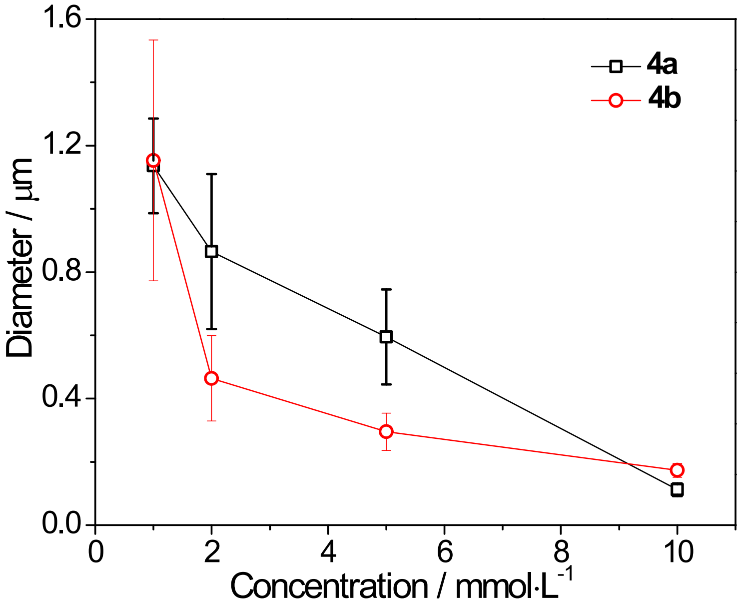

Fig. S5 Concentration-induced variation of the average size of the aggregates formed by **4a** and **4b** in $CHCl_3$.

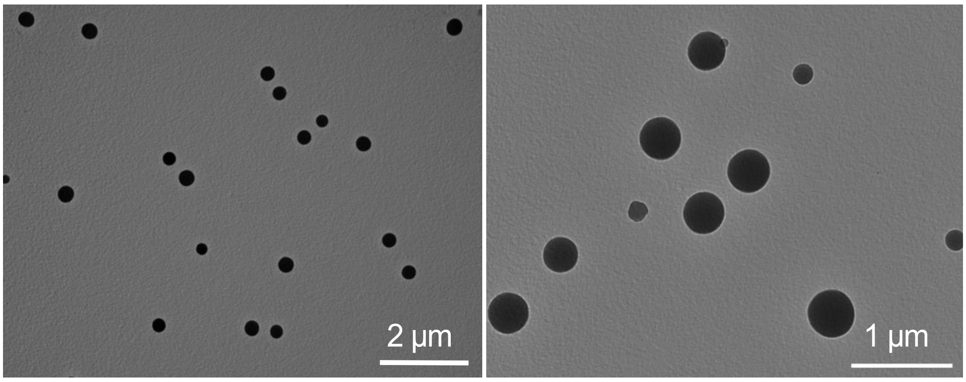

Fig. S6 Typical TEM images at different magnifications of the aggregates formed in **4a**$_{1.67\text{-}1.0}$-DMSO$_{40}$.

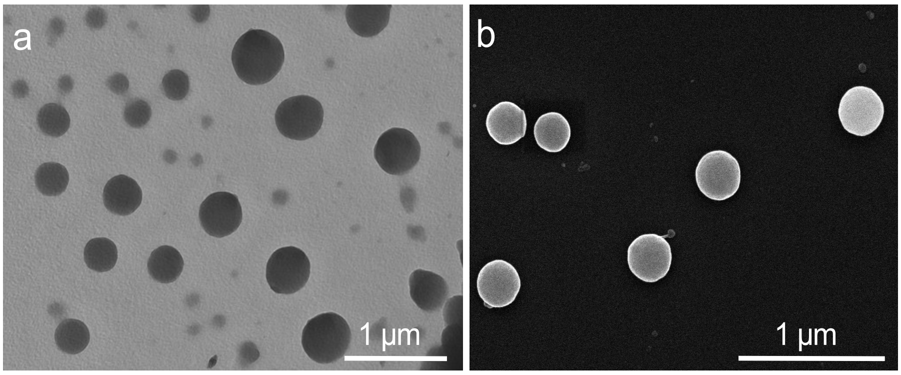

Fig. S7 Typical TEM (a) and SEM (b) images of the superstructures in the upper solution of **4a**$_{2.0\text{-}1.0}$-DMSO$_{50}$.

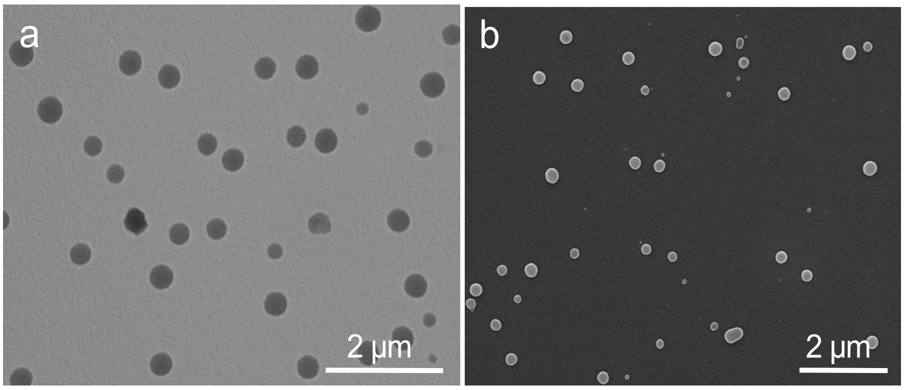

Fig. S8 Typical TEM (a) and SEM (b) images of the superstructures in the upper solution of $\mathbf{4a}_{2.5\text{-}1.0}$-DMSO$_{60}$.

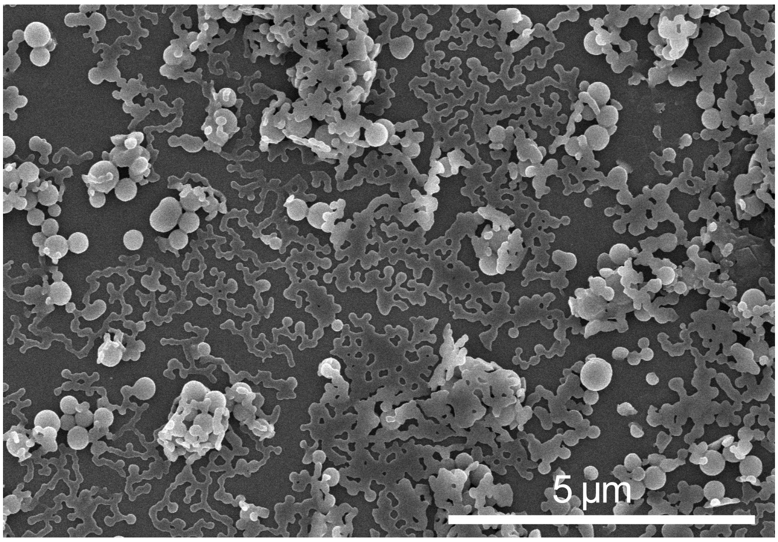

Fig. S9 A typical SEM image denoting the sphere-to-plate transition on silicon wafer in $\mathbf{4a}_{2.5\text{-}1.0}$-DMSO$_{60}$. Both intact spheres before transition and the transformed self-assemblies (plates) have been observed.

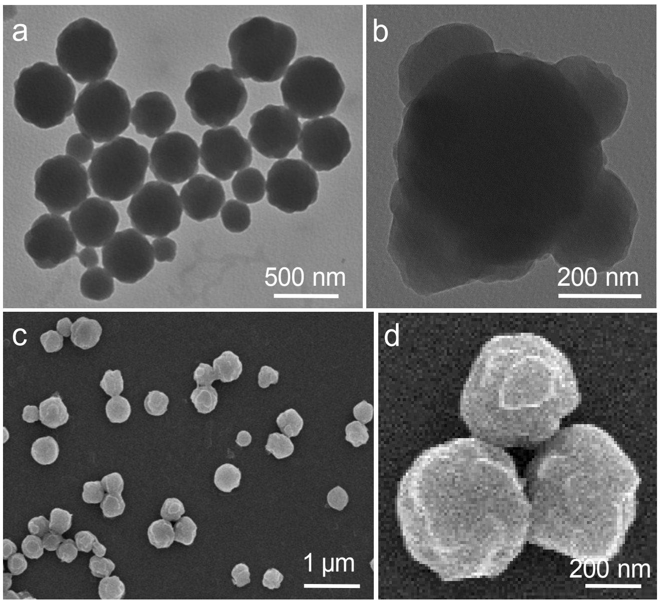

Fig. S10 Typical TEM (a, b) and SEM (c,d) images at different magnifications of the superstructures obtained from the bulk dispersion of $\mathbf{4a}_{5.0\text{-}1.0}$-DMSO$_{80}$.

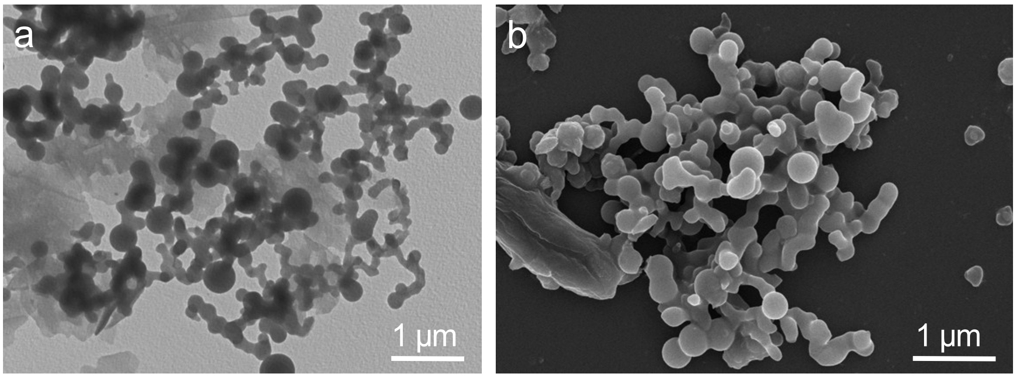

Fig. S11 Typical TEM (a) and SEM (b) images of the superstructures in the upper solution of $\mathbf{4a}_{10.0\text{-}1.0}$-DMSO$_{90}$.

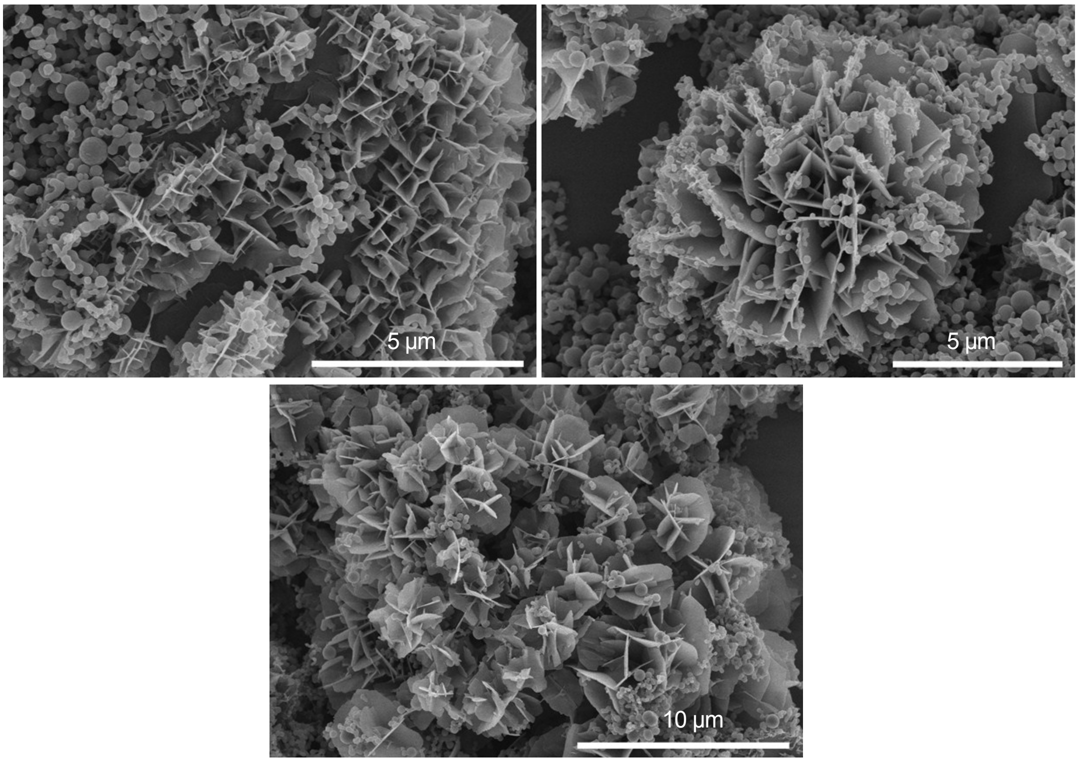

Fig. S12 Additional SEM images of the precipitates from $\mathbf{4a}_{10.0\text{-}1.0}$-DMSO$_{90}$.

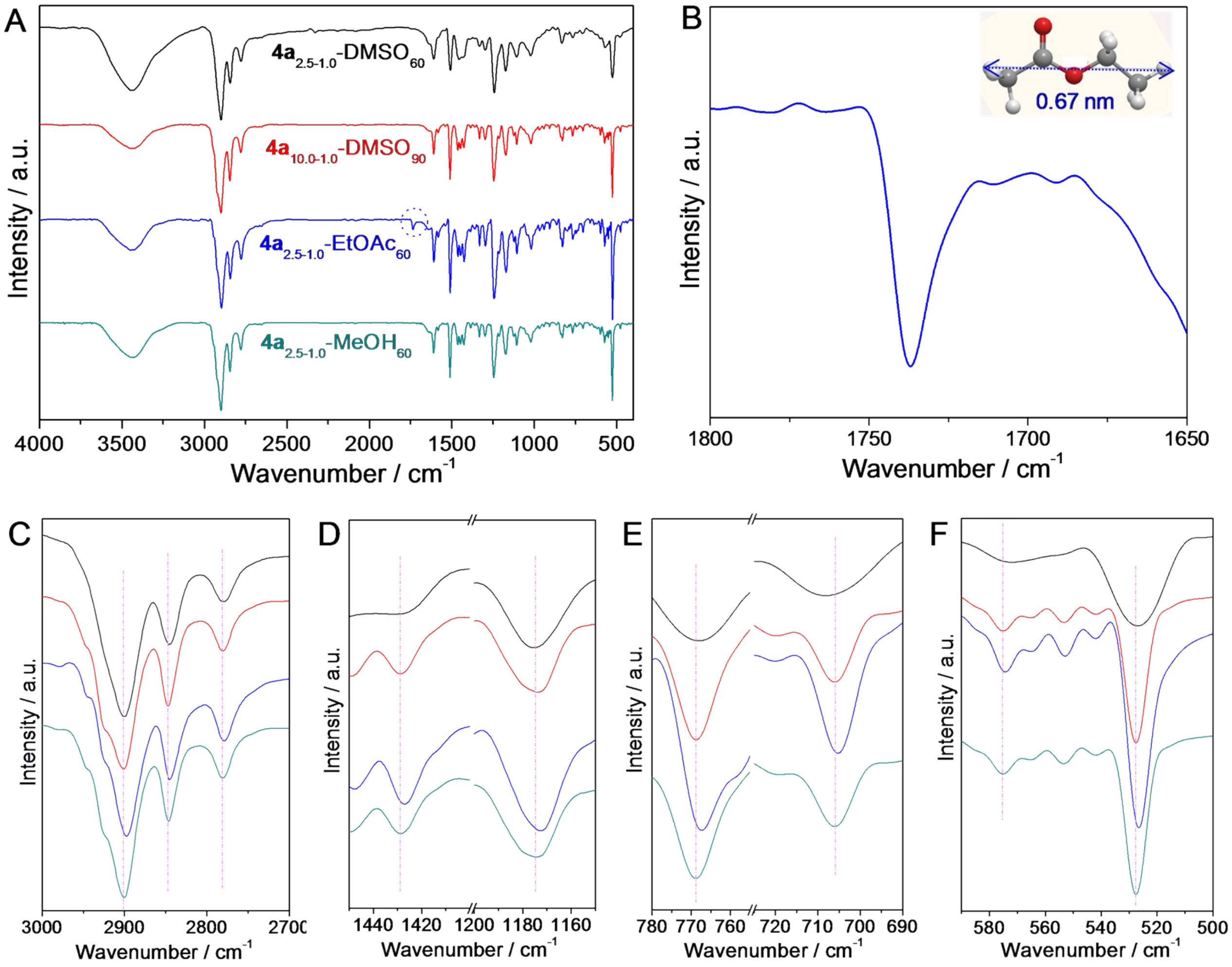

Fig. S13 FTIR spectra of the superstructures formed by **4a** in selected solvent combinations. A) An overview of the spectra. B) Magnified spectra of the marked region shown in A. Inset is the optimized conformation of EtOAc. C-F) Magnified spectra in selected wavelengths.

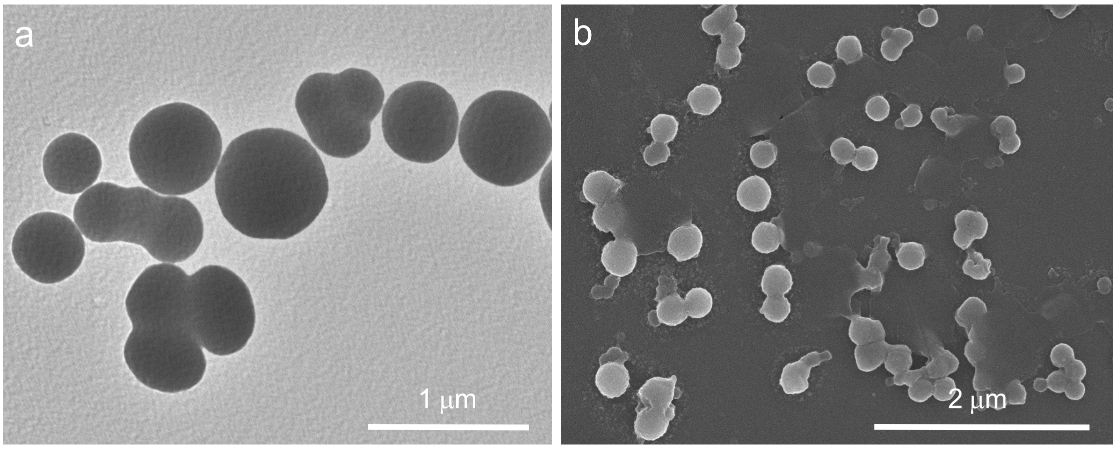

Fig. S14 Typical TEM (a) and SEM (b) images of the self-assemblies formed in $\mathbf{4b}_{2.0\text{-}1.0}$-DMSO$_{50}$.

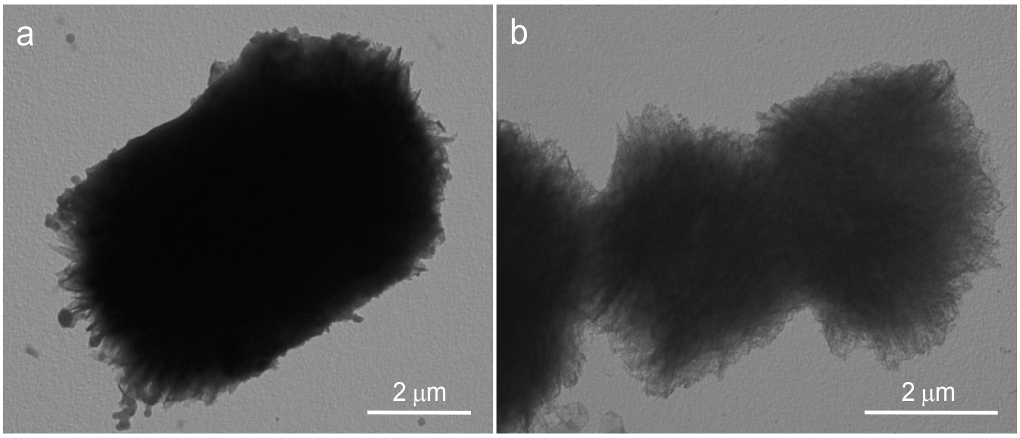

Fig. S15 Typical TEM images of the superstructures formed in $\mathbf{4b}_{2.5\text{-}1.0}$-DMSO$_{60}$ (a) and $\mathbf{4b}_{3.33\text{-}1.0}$-DMSO$_{70}$ (b).

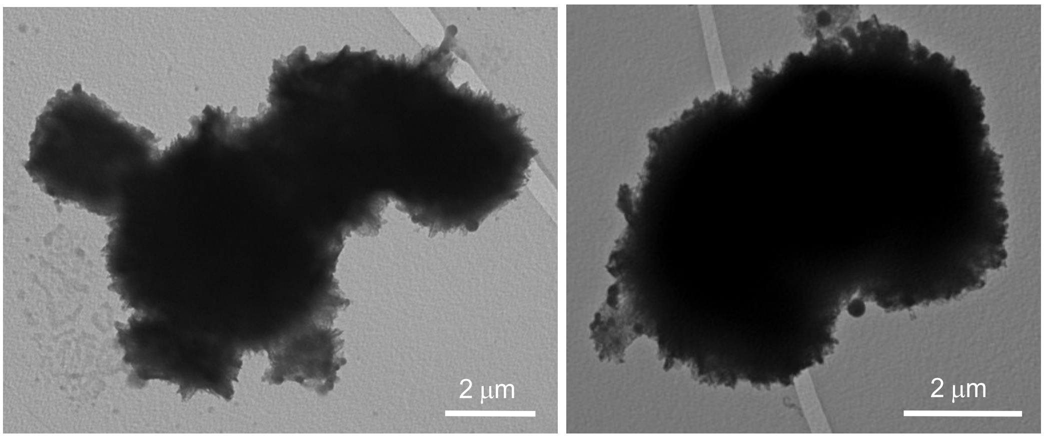

Fig. S16 Typical TEM images of the superstructures formed in $\mathbf{4b}_{5.0\text{-}1.0}$-DMSO$_{80}$.

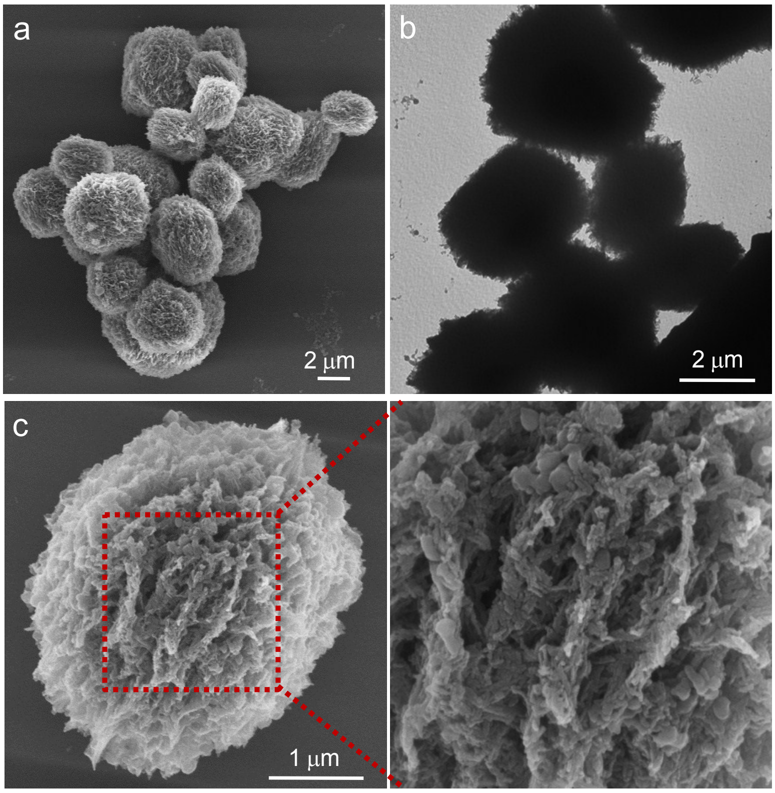

Fig. S17 Typical SEM (a, c) and TEM (b) images of the superstructures formed in $\mathbf{4b}_{10.0\text{-}1.0}$-DMSO$_{90}$.

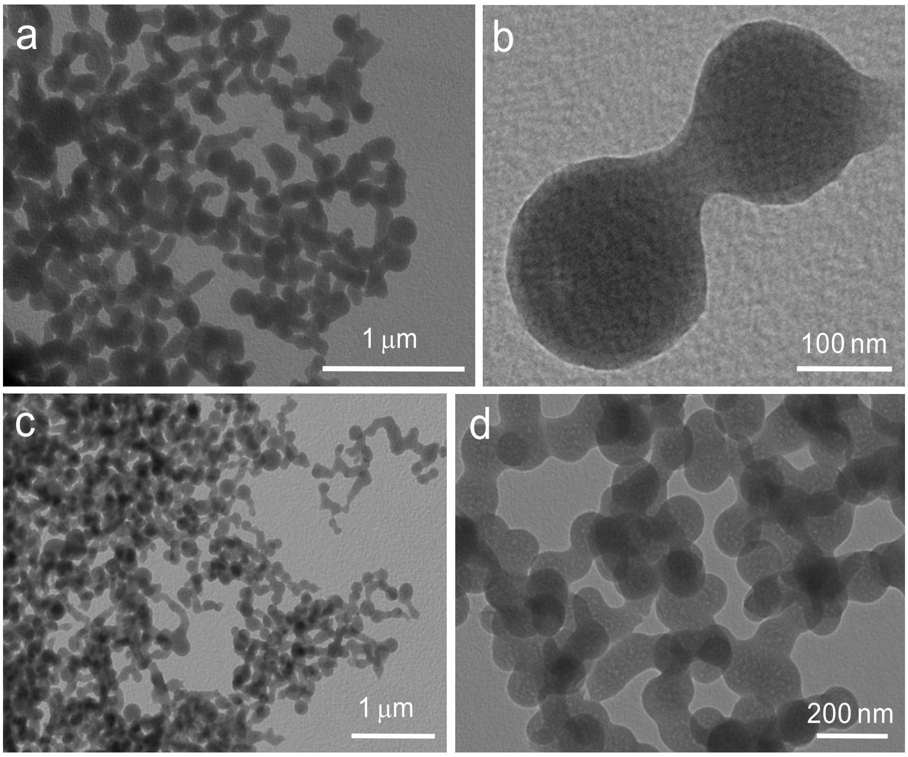

Fig. S18 Typical TEM images of the self-assemblies formed in the upper dispersion of **4b**$_{5.0\text{-}1.0}$-DMSO$_{80}$ (a, b) and **4b**$_{10.0\text{-}1.0}$-DMSO$_{90}$ (c, d).

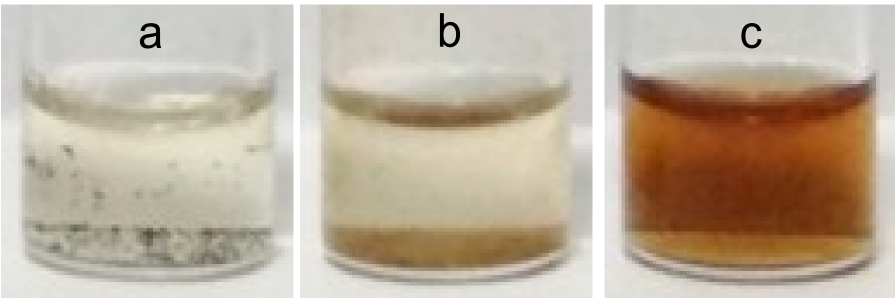

Fig. S19 Photoes of **4b**$_{2.5\text{-}1.0}$-acetone$_{60}$ (a), **4b**$_{2.5\text{-}1.0}$-MeOH$_{60}$ (b) and **4b**$_{2.5\text{-}1.0}$-EtOAc$_{60}$ (c).

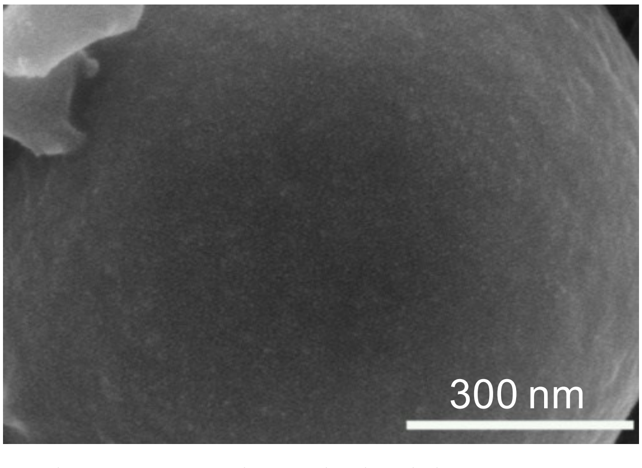

Fig. S20 A magnified SEM image on a sphere obtained from **4b**$_{1.25\text{-}0.5}$-MeOH$_{60}$ showing that the surface is relatively smooth.

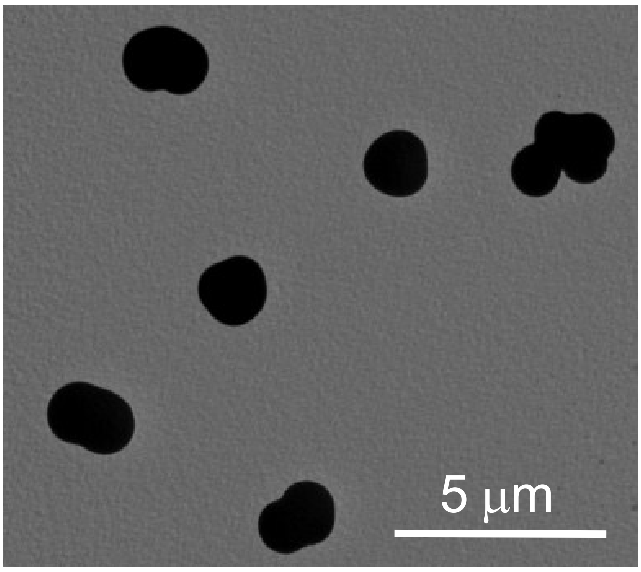

Fig. S21 A typical TEM image showing the solid character of the spheres obtained from **4b**$_{1.25\text{-}0.5}$-EtOAc$_{60}$.

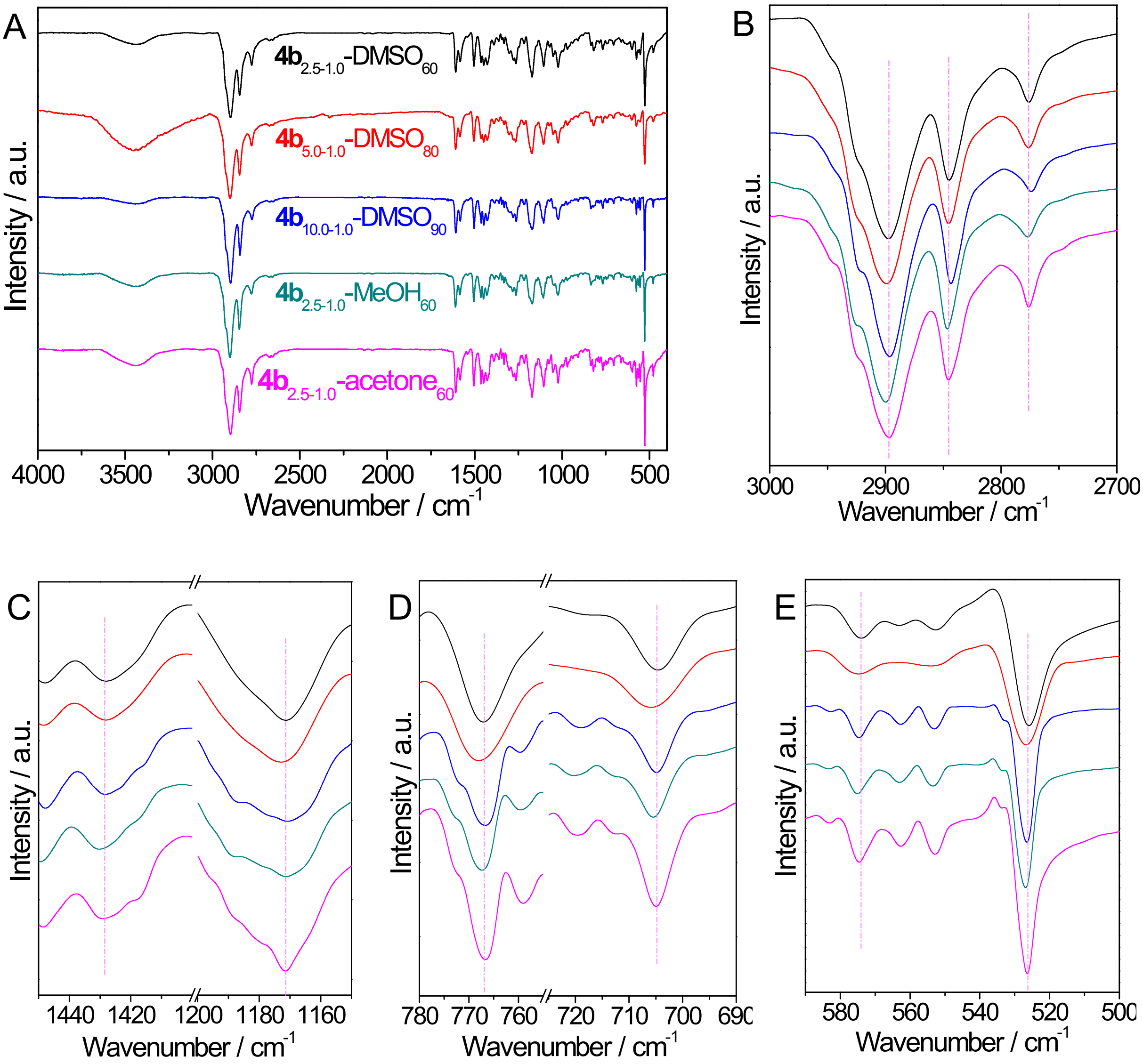

Fig. S22 FTIR spectra of the superstructures formed by **4b** in selected solvent combinations. A) An overview of the spectra. B-E) Magnified spectra in selected wavelengths.

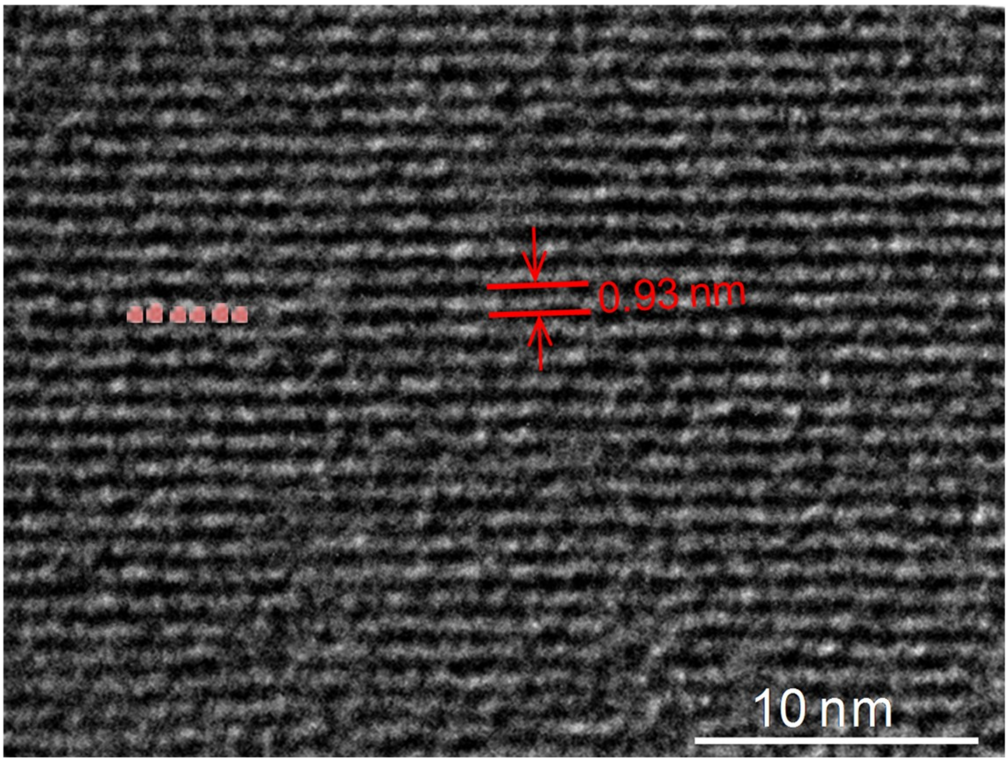

Fig. S23 A typical HRTEM image of the superstructures formed in **4a**$_{2.5\text{-}1.0}$-EtOAc$_{60}$.

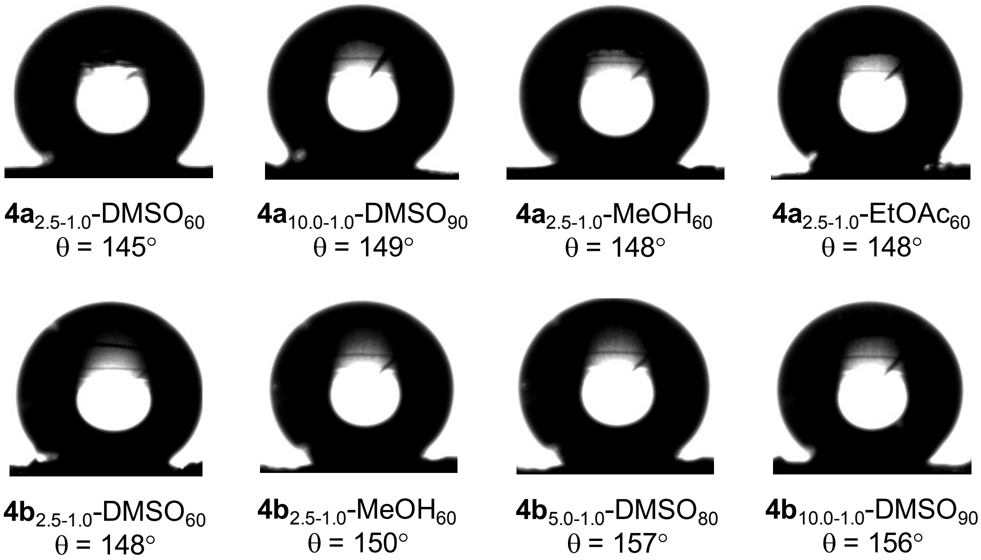

Fig. S24 Photos of water droplets on the surfaces of films prepared by the superstructures obtained from different samples.

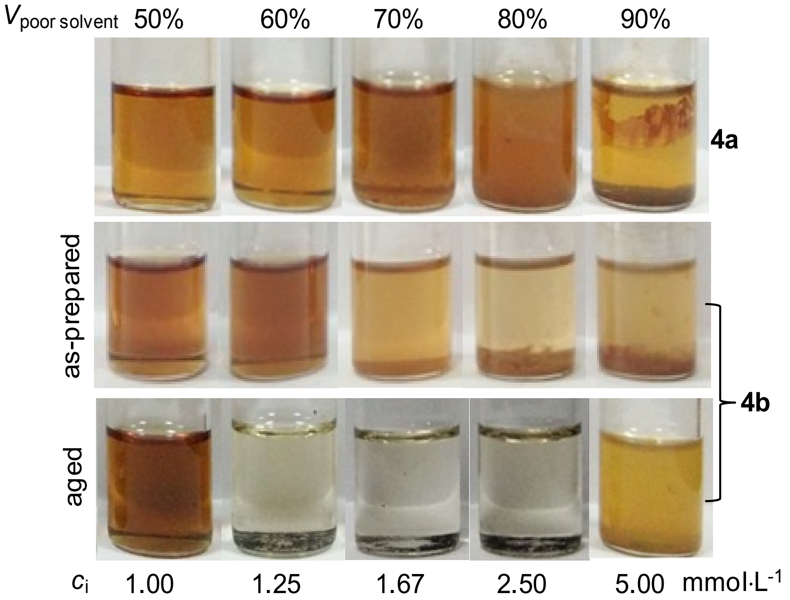

Fig. S25 Photos of typical samples in DMSO/$CHCl_3$ with c_f = 0.5 mmol·L^{-1}. The volume percentage of poor solvent and c_i are also included. Taken two weeks (the second row) or one month (the first and third rows) after sample preparation.

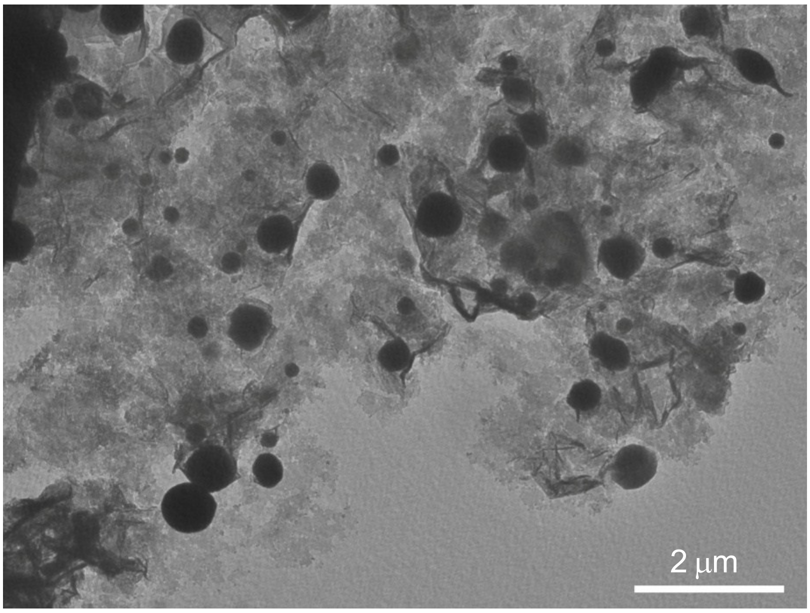

Fig. S26 A typical TEM image obtained from the precipitates in $\mathbf{4a}_{2.5\text{-}0.5}$-$DMSO_{80}$.

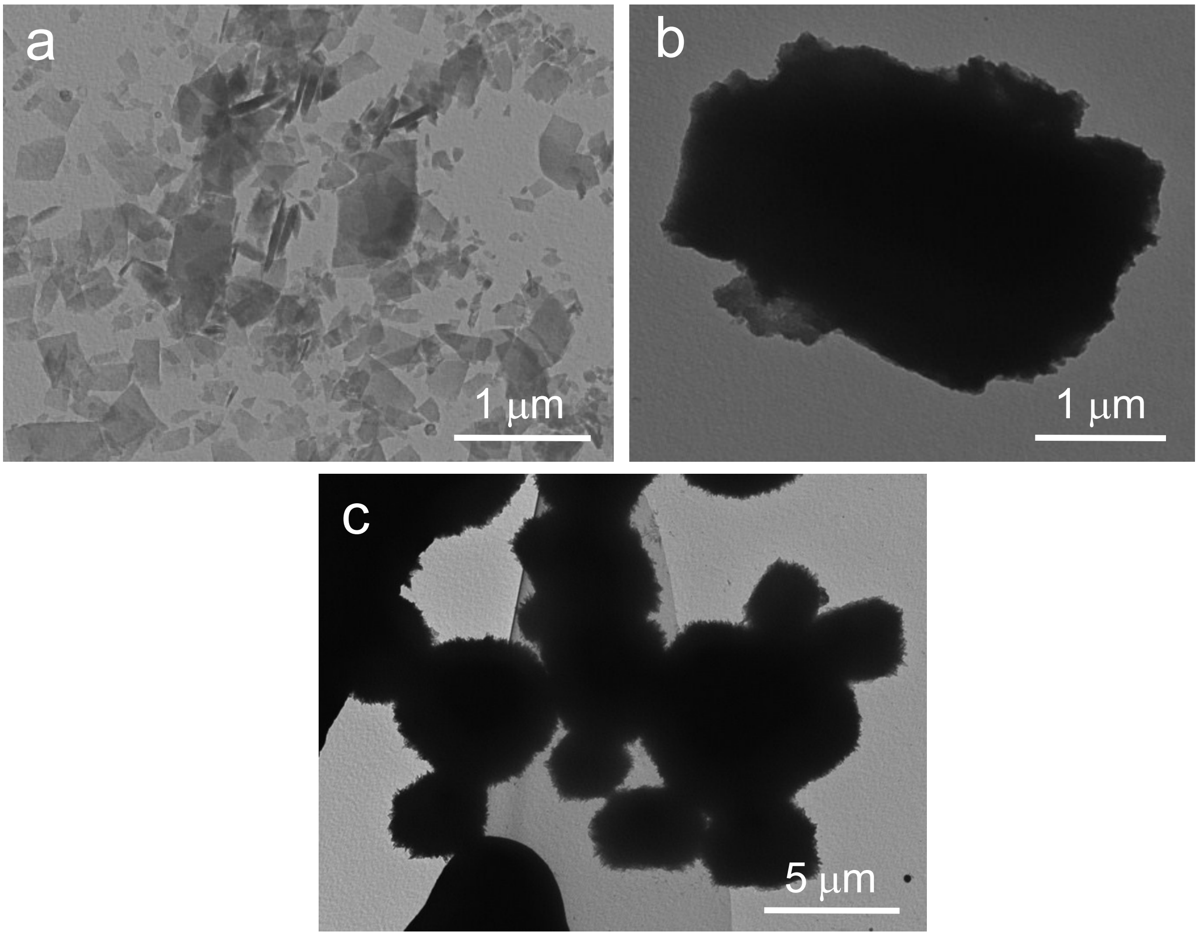

Fig. S27 TEM images obtained from the precipitates from **4b**$_{1.25\text{-}0.5}$-DMSO$_{60}$ (a), **4b**$_{1.67\text{-}0.5}$-DMSO$_{70}$ (b) and **4b**$_{2.5\text{-}0.5}$-DMSO$_{80}$ (c) showing the formation of randomly-stacked plates, block structures and plicated particles, respectively.